IChemE

0263–8762/99/$10.00+0.00

Trans IChemE, Vol 77 Part A, March 1999

AN EXPERIMENTAL STUDY OF INDIVIDUAL AIR BUBBLE ENTRAINMENT AT A PLANAR PLUNGING JET

P. D. CUMMINGS and H. CHANSON

Department of Civil Engineering, The University of Queensland, Australia

At the impact of a plunging liquid jet with a receiving pool, air bubbles may be entrained if the impact velocity exceeds a critical velocity. New experiments were performed in a two-dimensional plunging jet. The flow conditions near the inception of air entrainment were investigated. Two mechanisms of air entrainment were visualized at low jet velocities: by elongated air cavity and by foam bubbles. The breakage of entrained air bubbles was studied also. The results highlight that the bubble breakage process depends critically upon the initial bubble size.

Keywords: plunging jet; air entrainment; inception; bubble breakage; air-water flow

INTRODUCTION

When a water jet impacts a plunge pool, some air may be carried downwards. Examples of mechanical penetration of one phase into another include self aeration in free jets, high speed open channel flows, entrainment via surface vortices, drop impact, hydraulic jumps and breaking waves (e.g. Bin[1], Chanson[2]). Air entrainment by plunging jet is an industrially important process where air entrainment, during the pouring of one liquid into another, is to be avoided, or entrainment is desired but control (e.g. of bubble sizes) is necessary.

Past studies (e.g. Ervine and Elsawy[3], Lara[4]) showed that air bubble entrainment takes place when the jet impact velocity V exceeds a characteristic value V_e which is primarily a function of fluid properties, jet length and jet core turbulence. For $V > V_e$, air entrainment is observed by an individual bubble entrainment process for V slightly larger than V_e or by a ventilated cavity mechanism at larger jet impact velocities (Cummings and Chanson[5,6]). After being entrained, air bubbles may break up if the combination of fluid shear stresses and pressures exceed the surface tension forces.

Most studies of air entrainment inception and individual air bubble entrainment were performed with circular jets. Sene[7] (1988) studied sloping supported planar jets. In the present paper, the authors present an experimental study of plunging jet entrainment with a simple geometry, specifically a vertical supported plunging jet. The inception flow conditions and the individual bubble entrainment process were investigated using high-speed camera and video-camera, and the results are presented herein.

EXPERIMENTAL PROCEDURE

The experiment consists of a fresh water planar jet, 0.27 m wide and 0.012 m thick (Figure 1). The jet plunges into a 1.8 m deep, 0.3 m wide and 3.6 m long channel with glass walls (Figure 1(a)). The jet angle with the horizontal was set at 89° to ensure that the jet remained attached to the support. Although the jet angle affects the inception velocity[1], a 1-degree deviation from the vertical has very little influence. Discharges were measured with an orifice plate meter, and clear-water velocity and velocity fluctuations were recorded with a 3.3 mm Pitot tube.

A Panasonic™ F15 CCD WV-F15HSE Cam-corder video camera was used to visualize air bubble entrainment below the plunge pool surface. A 500 W tungsten bulb lamp was positioned on the far side of the channel to provide forward scattering illumination of the bubbles. The positions of the camera and lamp are shown in Figure 1(b) as well as a still photograph. Note the impingement perimeter and several entrained bubbles. The camera was equipped with a macro lens and used in strobe effect shutter (SES) mode: a frame was taken every 20 ms with a shutter speed of 500 μs. Each frame consists of a scan of alternate horizontal light sensor lines, with the following frame being a scan of the lines missed in the previous frame (interweaving). Scaling for the camera images was done by filming a spherical steel ball bearing of known diameter at various locations near the jet centre line. Bubbles outside of the ball bearing locations were out of focus and ignored. High-speed photographs were further taken with a 35 mm camera (35 μs shutter speed). Further information on the experimental setup and instrumentation is given by Cummings[8].

Experimental Setup and Procedure

Uniformity of the mean velocity across the jet width and thickness was checked and found to vary by +/− 1.1% outside of the support and side wall boundary layers. The air-water surface tension was measured using glass capillary tubes (ϕ = 1.2 to 3.2 mm) and found to be 0.055 N m^{-1} at 25°C.

(a)

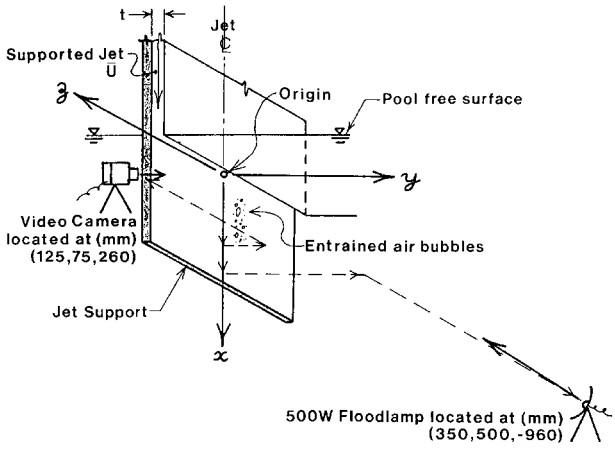

(b)

Figure 1. Experimental setup. (a) Side view of the supported plunging jet experiment (flow direction: top to bottom). $d = 0.012$ m, $V = 4.2$ m s^{-1}, $L_j = 0.1$ m. (b) High speed photograph and video camera arrangement (flow direction: top to bottom). The support is on the left. The coordinates are denoted (x, y, z).

Note two main assumptions used in the operation of the video camera and Pitot tube: [1] no air-water mass transfer occurred and [2] the Pitot tube was aligned with the fluid streamlines.

AIR ENTRAINMENT INCEPTION

The main results for the air entrainment inception conditions are summarized in Figure 2 and Table 1, where the onset velocity for air entrainment V_e is defined as the mean centreline jet velocity (outside the developing boundary-layer) at impact, Tu is the jet turbulence intensity, d is the jet thickness at impact and L_j is the length of the free-falling jet. The data indicate a decreasing inception velocity with increasing turbulence level. The trend is

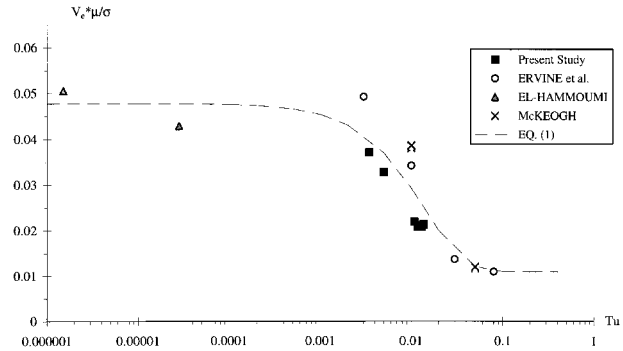

Figure 2. Vertical plunging jets air entrainment inception flow conditions. Comparison between experimental data and equation (1).

consistent with circular jet data (McKeogh[9], Ervine *et al.*[10], El-Hammoumi[11]) but it must be emphasized that the data depend critically upon the definitions of air entrainment inception and of the jet turbulence.

McKeogh, Ervine and El-Hammoumi recorded the jet turbulence at the nozzle but the authors measured Tu at impact and outside of the support boundary layer. McKeogh and Ervine defined Tu in terms of the longitudinal turbulent velocity fluctuation while El-Hammoumi recorded the turbulent velocity fluctuation in the direction normal to the jet flow (Table 1).

The authors observed consistently that inception is not a precise condition. A jet may entrain one or a few bubbles only every few minutes. Hence the selection of the investigation period (e.g. 1 or 10 minutes) is critical. Further, after being entrained, some rising bubbles stay on the surface of the plunge pool as foam bubbles, drifting towards the jet entrainment point. Such bubbles may then become attached to the jet/pool intersection for a period of time, before being re-entrained. Sometimes the re-entrainment caused by the surface foam bubbles consists of an air packet that is considerably larger than the original bubble and the 'primary' entrainment may be followed by numerous 'seconary' events until all of the bubbles have been cleared from the system.

In this study, the authors defined 'inception' as a 'primary' entrainment event which occurs within an interval of about 5 minutes, in the absence of bubbles in the plunge pool.

Discussion

Despite different definitions of 'inception' and of turbulence intensity, all the data (Figure 2, Table 1) show a consistent trend: i.e., V_e decreases with increasing Tu. At the limits, V_e tends to about 3.5 m s^{-1} for very-low turbulence jets ($Tu < 1$ E-5) and to 0.8 m s^{-1} for turbulent jets ($Tu > 0.1$). The dimensionless inception velocity of air-water plunging jets may be correlated by:

$$\frac{V_e \mu}{\sigma} = 0.0109 \, (1 + 3.375 \, \exp(-80 \times Tu)) \qquad (1)$$

where V_e is the jet impact velocity at inception, μ is the water dynamic viscosity and σ is the surface tension of air and water. Equation (1) is compared with data in Figure 2.

Table 1. Vertical supported planar plunging jet. Inception experimental data.

Reference (1)	V_e m s^{-1} (2)	Tu % (3)	L_j m (4)	d m (5)	Remarks (6)
Present study		$Tu = u'/V$			2-D jets ($\theta = 89$ deg.). $\sigma = 0.055$ N m^{-1} for all experiments.
	2.03	0.35	0.179	0.003	
	1.79	0.50	0.134	0.0035	
	1.2	1.08	0.034	0.008	
	1.17	1.36	0.005	0.010	
	1.15	1.21	0.017	0.009	
	1.14	1.19	0.037	0.006	
	1.14	1.30	0.028	0.0075	
McKeogh, 1978[9]		$Tu = u'/V_N$			ϕ jets ($\theta = 70$ deg.).
	0.85	0.05	0.005	0.00265	
	0.85	0.05	0.005	0.0058	
	0.87	0.05	0.005	0.0087	
	0.88	0.05	0.005	0.014	
	2.78	0.01	0.005	0.0027	
	2.81	0.01	0.005	0.0060	
	2.83	0.01	0.005	0.0090	
	2.82	0.01	0.005	0.0145	
Ervine *et al.*, 1980[10]		$Tu = u'/V_n$			ϕ jets ($\theta = 70$ deg.). $d = 6$, 9, 14 and 25 mm.
	3.6	0.003	0		
	2.5	0.01	0		
	1	0.03	0		
	0.8	0.08	0		
El-Hammoumi, 1994[11]		$Tu = v'/V_n$			ϕ jets ($\theta = 90$ deg.).
	3.14	2..8E-5	0.290	0.0073	
	3.70	1.5E-6	0.290	0.012	

Notes: d: jet thickness measured at impact; V_e: onset velocity measured at impact.

MECHANISMS OF LOW SPEED ENTRAINMENT (INDIVIDUAL AIR BUBBLE ENTRAINMENT)

At low jet velocities, air is entrained in the form of individual air bubbles. Photographic evidence highlights two main entrapment processes (at low impact velocity): (1) entrainment via an elongated air cavity and (2) entrainment via surface foam bubbles.

Air entrainment by elongated air cavity is illustrated in Figure 3. Firstly, an air pocket extends downwards from the jet-plunge pool intersection (Figure 3.1 and 3.2). Then the end of the cavity breaks off to form several individual bubbles (Figure 3.4 to 3.6). Sometimes the elongated air pocket (e.g. Figure 3.1 and 3.2) may be observed to retract without air bubble entrainment. Once, a cavity was observed to pulsate with a period of about 60 ms under a jet with $V = 1.17$ m s^{-1}, $Tu = 1.36$ %, $d = 10.0$ mm and $L_j = 5$ mm. The analysis of video-camera pictures indicates that the elongated air cavities are about 7 to 18 mm long and the transverse dimension (in plane normal to flow direction) is about 1.0 to 4.5 mm. Generally elongated air cavities are observed to occur under areas of high free surface roughness on the impinging jet.

Figure 4 illustrates air bubble entrainment by surface foam bubble being trapped at the jet-plunge pool intersection. These trapped bubbles perturb the flow sufficiently for bubbles to be entrained. Sometimes the number of surface foam bubbles is significant and a foam layer exists at the pool free-surface. Note that tap water was used and small quantities of surfactants were expected although their quantity was not measured.

Other forms of air bubble entrainment may be sometimes observed. Surface foam can be entrained, air contained within the jet body can be carried under the plunge pool surface, and small bubbles are entrained possibly via small surface cavities.

At higher jet velocities, the mechanisms of air bubble entrainment are very different (e.g., Chanson and Cummings[12], Chanson[2]).

BUBBLE BREAKAGE MECHANISMS WITH LOW-VELOCITY PLUNGING JET

After entrainment/entrapment at the jet-pool intersection, air bubbles are carried away in a developing shear layer in which bubble breakage may occur if the combination of fluid shear stresses and pressures exceed the surface tension forces. Several researchers used a criteria for breakage based upon a critical Weber number (e.g., Hinze[13], Sevik and Park[14], Lewis and Davidson[15]). But such a formulation assumes a uniform turbulent shear stress distribution which is untrue in a mixing layer.

Experimental Observations

New observations of bubble breakage were recorded with flow conditions near inception (i.e., $V \geq V_e$): i.e., from $V = 1.17$ m s^{-1}, $Tu = 1.38$%, $d = 10.0$ mm and $L_j = 5$ mm, to $V = 2.03$ m s^{-1}, $Tu = 0.35$%, $d = 3.0$ mm, $L_j = 179$ mm. Most bubble breakage events were observed between $x = 50$ and 100 mm, for which the shear layer width, measured between 10% and 90% of the free-stream velocity, was about 14 to 24 mm.

Figures 5 and 6 illustrate two bubble breakage sequences. Figure 5 shows the breakup of a 4 mm air pocket which

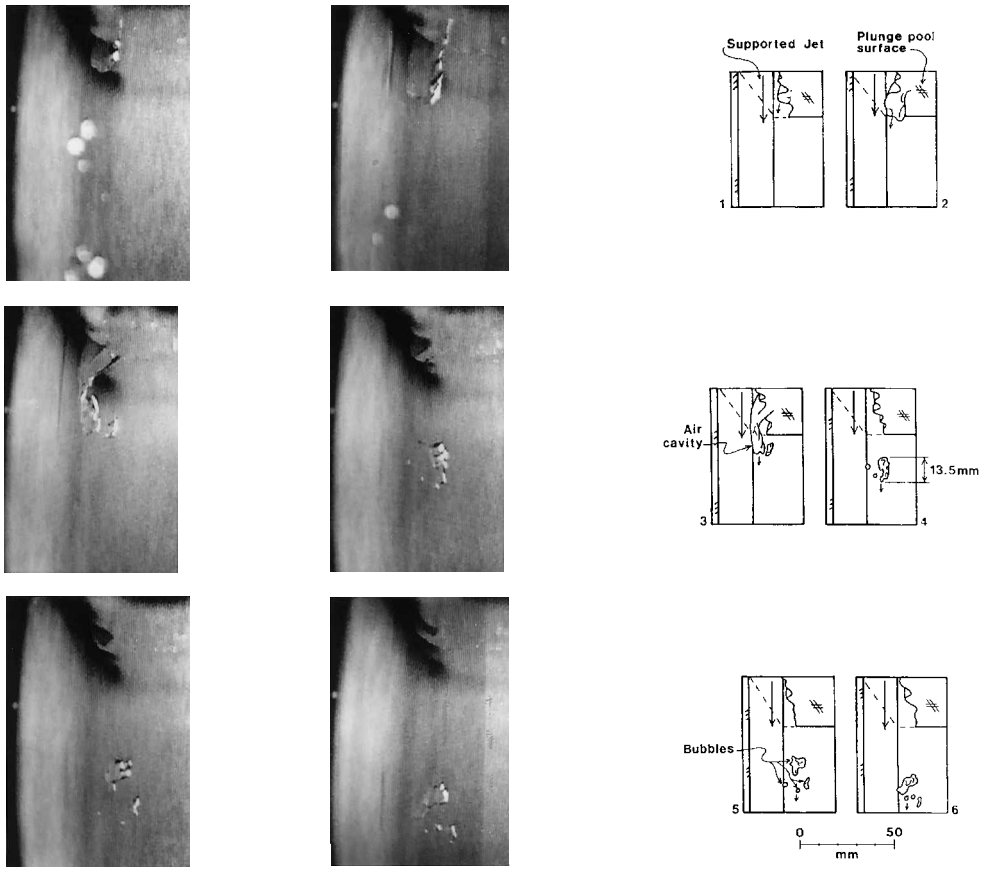

Figure 3. Low-speed air bubble entrainment. Elongated air cavity formation and entrainment of bubbles. Flow direction from top to bottom. Cavity and scaling located 45 mm towards the camera from the jet centre line. $V = 1.20\ m\ s^{-1}$, $Tu = 1.08\ \%$, $d = 8.0$ mm, $L_j = 34$ mm. Video shutter speed: 1.0 ms, frame interval: 20 ms.

splits into two roughly equal-sized pockets. In Figure 6, two large elongated bubbles split into three products in one case and two differently sized products in the other case.

For a large number of single-bubble breakages (Table 2), the number and size of 'daughter' particles were recorded (Figures 7 and 8). In the study, a breakage is defined as an event that occurred between two successive video frames (i.e. a 20 ms period) and, for each experiment, the apparent bubble diameter D is the average of the measured bubble major- and minor-axes lengths. Figure 7 shows the number of post-breakage bubbles per original bubble ('parent-bubble') for three ranges of parent bubble diameters D. The results illustrate that most smaller bubbles break into two particles whereas the breakage of larger bubbles ($D > 10.5$ mm) tend to give on average 2.7 daughter bubbles. Such a result might result from different modes of breakage with different 'parent-bubble' size (see Discussion).

Table 2. Single-bubble breakage sampling (present study).

D mm (1)	Sample size Nb of experiments (2)
1.5–5.5	147
5.5–10.5	40
>10.5	11

Note: D apparent bubble size of the 'mother' (original) bubble.

Figure 8 presents experimental observations of 'daughter' bubble sizes, presented as the ratio of post- to pre-breakage bubble size. Each histogram column represents the probability of the ratio D_{post}/D_{pre} in a 0.2 interval: e.g., the column 0.8 indicate the probability of $0.8 < D_{post}/D_{pre} \leq 1$. For small bubbles ($D_{pre} < 5.5$ mm), the daughter bubbles are on average 2.3 times smaller than the parent-bubble while, with the largest bubbles ($D_{pre} > 10.5$ mm), the ratio D_{post}/D_{pre} is predominantly less than 0.2.

Discussion

Firstly, the sum of the pre-breakage and post-breakage bubble volumes were compared to check the continuity for air. The post- to pre-volume ratio (for data in Figure 8) is 74.7%, which is reasonable considering the difficulties in estimating bubble sizes from two-dimensional video pictures.

Secondly, the authors are able to hypothesize several breakage mechanisms depending upon the parent-bubble size, based on video-camera pictures. Most small bubbles ($D = 1.5$ to 5.5 mm) tend to form a 'kidney shape' before breaking into predominantly two particles. The medium-size bubbles ($D = 5.5$ to 10.5 mm) stretch typically into an 'S-shape'. With large bubbles ($D > 10.5$ mm), the bubble

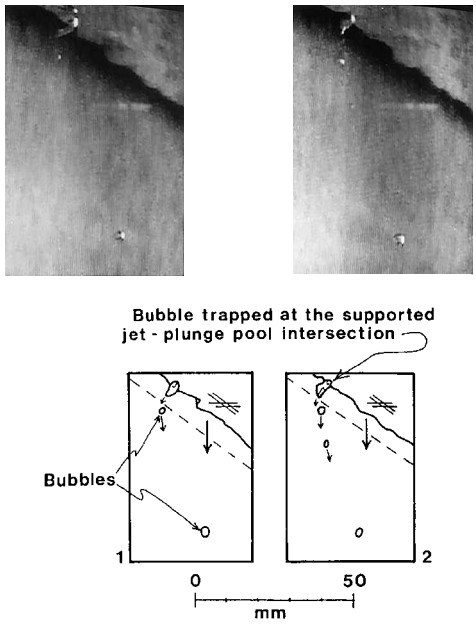

Figure 4. Air bubble entrainment caused a trapped surface bubble. Flow direction from top to bottom. Trapped bubbles and scaling located at the jet centre line, $V = 1.20\,\mathrm{m\,s^{-1}}$, $Tu = 1.08\%$, $d = 8.0\,\mathrm{mm}$, $L_j = 34\,\mathrm{mm}$. Video shutter speed: 1.0 ms, frame interval: 20 ms.

deformation forms an elongation extending some distance from the bubble gravity centre until the extremity breaks off to form several smaller bubbles ('tip-streaming'). The hypothesis is consistent with the observations that larger bubbles produce more breakage products (i.e. daughter bubbles) than small bubbles. To some extent, the observed mechanism are similar to observations of drop breakage by others (e.g., De Bruin[16]).

Overall the authors' results indicate fewer bubble breakage products than Pandit and Davidson[17]. Pandit and Davidson used orifice flows (25 to 35 mm orifice ϕ) and they observed breakages of 2.5 to 12.4-mm bubbles injected upstream of and entrained in the orifice. The bubbles broke

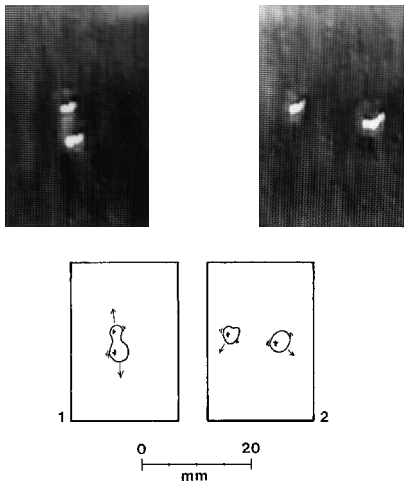

Figure 5. Bubble breakage at low-velocity plunging jet. $D = 4.0\,\mathrm{mm}$. Flow direction from top to bottom. Bubble breakage at: $x = 25\,\mathrm{mm}$, $y = 12\,\mathrm{mm}$, $z = 0$. Flow conditions: $V = 1.14\,\mathrm{m\,s^{-1}}$, $Tu = 1.19\%$, $d = 6.0\,\mathrm{mm}$, $L_j = 37\,\mathrm{mm}$. Video shutter speed: 1.0 ms, frame interval: 20 ms.

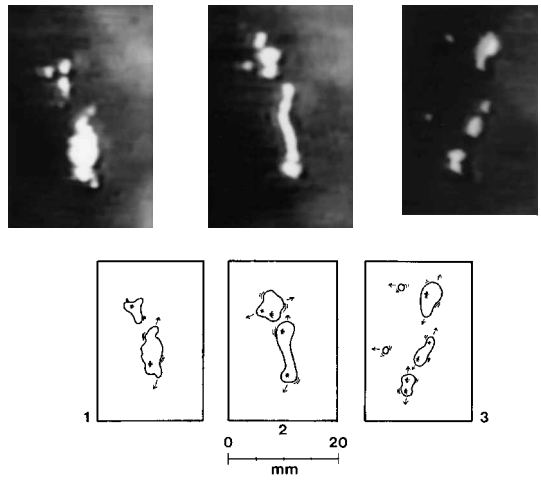

Figure 6. Bubble breakage at low-velocity plunging jet. Flow direction from top to bottom. Bubble elongation and breakage at: $x = 40\,\mathrm{mm}$, $y = 12\,\mathrm{mm}$, $z = 0$. Flow conditions: $V = 1.14\,\mathrm{m\,s^{-1}}$, $Tu = 1.19\%$, $d = 6.0\,\mathrm{mm}$, $L_j = 37\,\mathrm{mm}$. Video shutter speed: 0.5 ms, frame interval: 20 ms.

in a fully developed jet that was thicker than the bubble diameters. With the authors' experiment, it was observed that some large bubbles were only partially effected by the shear layer and were subjected only to partial breakage by tip-streaming. It is believed that such bubbles were of a similar size as the width of the shear layer (i.e. 14 to 24 mm).

CONCLUSION

The inception of air bubble entrainment by a vertical supported planar plunging water jet has been investigated. Inception conditions of air-water flows depend critically upon the jet turbulence (equation (1), Figure 2). The inception velocity is nearly constant ($V_e = 0.8\,\mathrm{m\,s^{-1}}$) for rough-turbulent jets, while, with very-smooth turbulent jets ($Tu < 1\mathrm{E}\text{-}5$), V_e equals $3.5\,\mathrm{m\,s^{-1}}$.

At low jet velocities, two new mechanisms of air bubble entrainment are observed. An elongated air cavity mechanism is noted, associated with areas of large jet surface roughness. If the jet free-surface is exceptionally smooth, this mechanism may not be present until a higher jet speed

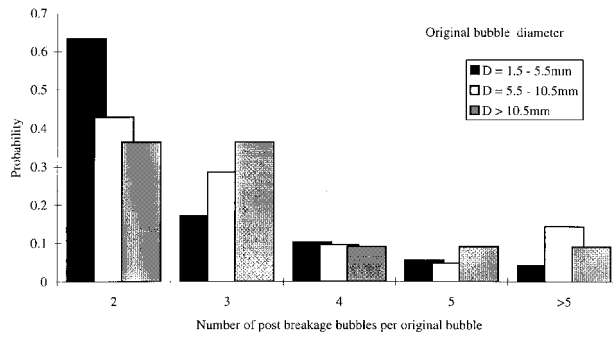

Figure 7. Single bubble breakage: number of breakage products/original bubble. Flow conditions ranging from $\{V = 1.17\,\mathrm{m\,s^{-1}}$, $Tu = 1.38\%$, $d = 10.0\,\mathrm{mm}$, $L_j = 5\,\mathrm{mm}\}$ to $\{V = 2.03\,\mathrm{m\,s^{-1}}$, $Tu = 0.35\%$, $d = 3.0\,\mathrm{mm}$, $L_j = 179\,\mathrm{mm}\}$.

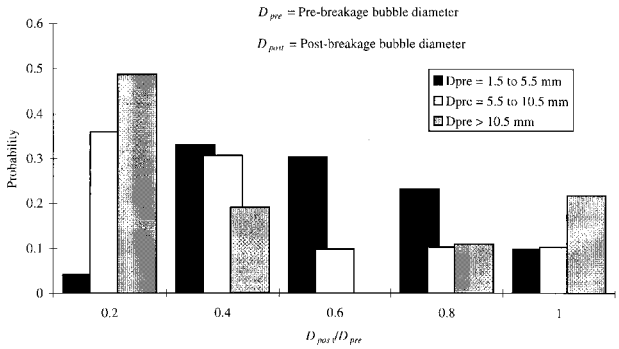

Figure 8. Single bubble breakage: post-breakage bubble spectra. Flow conditions ranging from $\{V = 1.17\,m\,s^{-1}$, $Tu = 1.38\%$, $d = 10.0\,mm$, $L_j = 5\,mm\}$ to $\{V = 2.03\,m\,s^{-1}$, $Tu = 0.35\%$, $d = 3.0\,mm$, $L_j = 179\,mm\}$.

is attained. Air entrainment was also observed to be caused by the presence of foam bubbles at the jet-plunge pool intersection.

Bubble breakage mechanisms were studied below the jet impingement point. Data indicate that the bubble breakage process is a function of the bubble size. Small bubbles ($D < 5.5\,mm$) are deformed into a kidney shape prior to breaking, splitting into two particles of nearly equal size. Larger bubbles were observed to stretch into elongated shapes prior to breakage.

The present study provides a new understanding of the low jet velocity entrainment process by plunging jet. However, the extension of the study to large jet velocity is necessary and new experimental techniques will be required.

LIST OF SYMBOLS

D	apparent bubble diameter defined as the average of the bubble major- and minor-axes length, m
D_{pre}	pre breakage bubble diameter, m
D_{post}	post bubble diameter, m
L_j	nozzle to plunge point jet length, m
d	jet thickness at impact, m
Tu	jet turbulence intensity defined as: $Tu = u'/V$ (present study), $Tu = u'/V_n$ (McKeogh, 1978[9], Ervine *et al.*, 1980[10]), $Tu = v'/V_n$ (El-Hammouni, 1994)[11]
u'	standard deviation of the axial velocity fluctuations about the mean, $m\,s^{-1}$
V	jet velocity at impact, $m\,s^{-1}$
V_e	onset velocity for air entrainment measured at jet impact, $m\,s^{-1}$
V_n	nozzle velocity, $m\,s^{-1}$
v'	standard deviation of the normal velocity fluctuations about the mean, $m\,s^{-1}$
x	distance in the direction of the jet's mean flow, measured from the jet impact point, m
y	distance normal to the jet's support, m
z	distance normal to the x-y plane measured from the jet centre line, m

Greek letters

μ	dynamic viscosity of water, Pa s
θ	jet angle with horizontal
σ	surface tension, $N\,m^{-1}$

REFERENCES

1. Bin, A. K., 1993, Review article No. 43—Gas entrainment by plunging liquid jets, *Chem Eng Sci*, 48 (21): 3585–3630.
2. Chanson, H., 1997, *Air Bubble Entrainment in Free-Surface Turbulent Shear Flows* (Academic Press, London, UK) 401 pages.
3. Ervine, D. A. and Elsawy, E. M., 1975, The effect of falling nappe on river aeration, *Proc 16th IAHR Congress, Sao Paulo, Brazil*, Vol. 3, p. 390.
4. Lara, P., 1979, Onset of air entrainment for a water jet impinging vertically on a water surface, *Chem Eng Sci*, 34: 1164–1165.
5. Cummings, P. D. and Chanson, H., 1997, Air entrainment in the developing flow region of plunging jets. Part 1: Theoretical development, *J Fluids Eng, Trans ASME*, 119 (3): 597–602.
6. Cummings, P. D. and Chanson, H., 1997, Air entrainment in the developing flow region of plunging jets. Part 2: Experimental. *J Fluids Eng, Trans ASME*, 119 (3): 603–608.
7. Sene, J. K., 1988, Air entrainment by plunging jets, *Chem Eng Sci*, 43 (10): 2615–2623.
8. Cummings, P. D., 1996, Aeration due to breaking waves, *PhD Thesis*, (University of Queensland, Brisbane, Australia) 230 pages.
9. McKeogh, E. J., 1978, A study of air entrainment using plunging water jets, *PhD Thesis* (Queen's University of Belfast, UK) 374 pages.
10. Ervine, D. A., McKeogh, E. J. and Elsawy, E. M., 1980, Effect of turbulence intensity on the rate of air entrainment by plunging water jets, *Proc Inst Civil Eng*, Part 2, June, pp. 425–445.
11. El Hammouni, M., 1994, Entraînement d'air par jet plongeant vertical. Application aux becs de remplissage pour le dosage pondéral. Air entrainment by vertical plunging jet. Application to refill nozzles applied to doage, *PhD Thesis* (INPG, Grenoble, France (in French)).
12. Chanson, H. and Cummings, P. D., 1994, An experimental study on air carryunder due to plunging liquid jet—discussion, *Int J of Multiphase Flow*, 20 (3): 667–770.
13. Hinze, J. O., 1955, Fundamentals of the hydrodynamic mechanism of splitting in dispersion processes. *AIChE J*, 1 (3): 289–295.
14. Sevik, M. and Park, S. H., 1973, The splitting of drops and bubbles by turbulent fluid flow, *J Fluids Eng, Trans ASME*, March, pp. 53–60.
15. Lewis, D. A. and Davidson, J. F., 1982, Bubble splitting in shear flow, *Trans IChemE*, 60: 283–291.
16. De Bruin, R. A., 1993, Tipstreaming of drops in simple shear flows, *Chem Eng Sci*, 48 (2): 277–284.
17. Pandit, A. B. and Davidson, J. F., 1986, Bubble breakup in turbulent liquid, *Int Conf on Bioreactor Fluid Dynamics, Cambridge, UK*, Apr. 15–17, pp. 109–120.

ACKNOWLEDGEMENTS

The authors wish to thank particularly Professor C. J. Apelt, University of Queensland, who supported this project since its beginning. They acknowledge the support of the Department of Civil Engineering at the University of Queensland which provided the experimental facility, and the financial support of the Australian Research Council (Ref. No. A89331591). The first author was supported by an Australian Postgraduate Research Award during his PhD thesis.

ADDRESS

Correspondence concerning this paper should be addressed to Dr H. Chanson, Department of Civil Engineering, The University of Queensland, Brisbane, Queensland 4072, Australia. (E-mail: h.chanson@mailbox.uq.edn.au). Correspondence before 20 June 1999 to Department of Architecture and Civil Engineering, Toyohashi University of Technology, Toyohashi 441-8580, Japan). P. D. Cummings is now at Kinhill Engineers, PO Box 1197, Milton, Brisbane 4064, Australia.

The manuscript was received 14 April 1998 and accepted for publication after revision 15 December 1998.